17th World Conference on Earthquake Engineering, 17WCEE
Sendai, Japan - September 13th to 18th 2020

Simulation of Strong Ground Motion Distribution by Synthesis of Orthogonal Modes Decomposed from Scenario Shaking Maps

Y. Takahashi[(1)], N. Nojima[(2)] and M. Kuse[(3)]

[(1)] *Graduate Student, Graduate School of Natural Science and Technology, Gifu University, E-mail: yuki.takahashi.0828@gmail.com*

[(2)] *Professor, Dept. of Civil Engineering, Gifu University, E-mail: nojima@gifu-u.ac.jp*

[(3)] *Associate Professor, River Basin Research Center, Gifu University, E-mail: kuse@gifu-u.ac.jp*

Abstract

In prediction of seismic intensity distribution for a scenario earthquake, several cases of source parameter setting are usually adopted in order to incorporate epistemic uncertainty associated with various source effects. Spatial correlation in seismic intensity distributions is an important consideration especially for evaluation of seismic damage and risk of spatially distributed networks and portfolio of an inventory of facilities, since assumption of perfect (or no) correlation leads to over-estimation (or under-estimation) of variation. In addition, a number of shaking maps should be considered in order to take account of wide variety of possible situations. However, only a small number of shaking maps considering limited cases are available in general. In the previous study, the authors proposed a mode decomposition method to evaluate spatial variation and correlation reflected in a set of seismic intensity distribution maps by use of singular value decomposition technique. Furthermore, a simulation method was proposed to generate a number of seismic intensity distributions by synthesis of orthogonal modes decomposed from scenario shaking maps.

In order to examine the applicability, in this study, the proposed methods were applied to two kinds of scenario earthquakes which can be potentially caused by strike-slip faults: the South Western segment of the main part of the Yamasaki Fault Zone and the Central North segment of Fault Zone of the Itoigawa-Shizuoka Tectonic Line, whose number of cases are four and eight, respectively. The results of mode decomposition reveal that spatial variation and correlation of Mode 1 represents the characteristic distributions of mean seismic intensity reflecting the attenuation effect due to source-to-site distance and the amplification effect of subsurface ground. Spatial variation and correlation of Mode 2 represents the forward directivity effect. Areas showing positive and negative correlation are spatially divided into two, which is considered to be a typical feature to strike-slip fault rupture. The tendencies observed in Mode 1 and 2 are common to two scenario earthquakes of strike-slip faults. The higher modes, however, show complex distributions reflecting differences in allocation of asperities, and different tendencies are observed for the two scenario earthquakes.

By synthesizing orthogonal modes obtained using singular value decomposition, Monte Carlo simulations were performed. It is shown that the proposed method is capable to generate an arbitrary number of cases of seismic intensity distribution maps preserving the spatial variation and correlation in original set of shaking maps. Spatial correlation between a pair of two sites located in the same direction with regard to rupture propagation shows positive correlation. On the contrary, a pair of two sites located in the opposite direction shows negative correlation. These results were found to be dominantly attributed to above-mentioned Mode 2 representing spatial correlation due to forward directivity effect. The simulated distributions of seismic intensity can be conveniently used for damage and risk assessment taking spatial correlation into account.

Keywords: Seismic intensity distribution, Spatial variation and correlation, Singular value decomposition, Simulation

1. Introduction

Variations of predicted seismic intensity distribution arise from epistemic uncertainty, such as source effects, propagation path effects and site effects. In seismic hazard maps for specified seismic source faults (scenario earthquake shaking maps) published by the Headquarters for Earthquake Research Promotion [1] and Japan Seismic Hazard Information Site (J-SHIS) [2] established by the National Research Institute for Earth Science and Disaster Resilience, several cases of source parameter settings are adopted in order to incorporate epistemic uncertainty associated with prediction results. When a variety of seismic intensity maps with different fault parameter settings for a given scenario earthquake is considered, spatial correlation shows significantly complicated distribution including negative values, affected by radiation patterns and rupture propagation effect such as directivity effect.

In evaluating seismic risk of spatially distributed networks or portfolio risk of an inventory of buildings, the simultaneous damage of buildings located at different sites is an important consideration. The occurrence of simultaneous damage is strongly related to spatial correlation in seismic intensity distributions. In evaluating seismic risk, assuming spatial correlation between sites to be complete (or no) correlation result in over-estimation (or under-estimation) of variation. In addition, a number of shaking maps should be considered in order to take account of wide variety of possible situations. However, only a small number of shaking maps considering limited cases are available in general. Therefore, seismic risk assessment requires simulation of seismic intensity distributions preserving spatial correlation, and integration of individual evaluation results.

There are many studies being performed in order to evaluate spatial correlation in strong ground motion distributions [3, 4, 5] and generate strong ground motion distributions considering spatial correlation [4, 5]. The functions of site-to-site correlation were modeled by separation distance based on the records of the 1999 Chi-Chi earthquake in Taiwan that was studied by Takada et al. [3], and the records of earthquakes in Kanto district of Japan that were studied by Hayashi et al. [4]. Furthermore, Hayashi et al. [4] proposed a simulation method for spatial correlation of ground motion intensity based on the correlation coefficient matrix with site-to-site correlation as an entry. The spatial correlation functions are modeled assuming spatial homogeneity (uniformity and isotropic) of variation. Therefore, it is not appropriate to apply the function to a set of Scenario Earthquake Shaking Maps of which variation varies spatially depending on the source parameter settings.

In the previous studies [6, 7], the authors proposed a mode decomposition method to evaluate spatial variation and correlation reflected in a set of seismic intensity distribution maps by use of singular value decomposition technique. Furthermore, a simulation method for seismic intensity distributions preserving the spatial variation and correlation in original dataset by use of mode synthesis was proposed [6]. In this study, in order to examine the applicability, the proposed methods were applied to two kinds of scenario earthquakes which can be potentially caused by strike-slip faults: the South Western segment of the main part of the Yamasaki Fault Zone and the Central North segment of Fault Zone of the Itoigawa-Shizuoka Tectonic Line, whose number of cases are four and eight, respectively. The results of mode decomposition reveal the dominant factor of spatial variation and correlation reflected in two kinds of scenario earthquakes. In addition, it is shown that the proposed method is capable of generating an arbitrary number of cases of seismic intensity distribution maps preserving the spatial variation and correlation in original set of shaking maps. The seismic intensity distribution maps used in this study are Scenario Earthquake Shaking Maps published by J-SHIS [2], and seismic intensity is represented by the Japan Meteorological Agency (JMA) seismic intensity scale. The analytical results depend on the prediction method of the seismic intensity distribution, the source parameter settings, the number of cases, and the dataset.

2. Mode Decomposition using Singular Value Decomposition

Let x denote a variable representing seismic intensity, and seismic intensity map consisting of M grid cells is represented by a column vector $\mathbf{x}=(x_1, \ldots, x_M)^{\mathrm{T}}$. Thus, seismic intensity distributions maps for N cases of different parameter settings are described by the $M\times N$ matrix $\mathbf{X}$ as follow:

$$\mathbf{X}=\left(\mathbf{x}_1,\ldots,\mathbf{x}_N\right)=\begin{pmatrix} x_{11} & \cdots & x_{1N} \\ \vdots & \ddots & \vdots \\ x_{M1} & \cdots & x_{MN} \end{pmatrix} \tag{1}$$

where x_{ij} is seismic intensity at the site j in the seismic intensity distribution of Case i.

Then the matrix $\mathbf{X}$ is normalized by using the mean value μ_G and the standard deviation value σ_G of all N cases of seismic intensity maps. The normalized matrix is expressed as Eq.(2).

$$\mathbf{X_0}=\frac{\mathbf{X}-\mu_G\mathbf{H}}{\sigma_G} \tag{2}$$

$$\mu_G=\frac{\sum_{i=1}^{M}\sum_{j=1}^{N}x_{ij}}{MN} \qquad \sigma_G=\sqrt{\frac{\sum_{i=1}^{M}\sum_{j=1}^{N}\left(x_{ij}-\mu_G\right)^2}{MN}} \tag{3}$$

where $\mathbf{H}$ is the $M\times N$ matrix in which all of entries are 1. Next, Singular value decomposition is applied to the matrix $\mathbf{X_0}$ [6].

$$\mathbf{X_0}=\mathbf{UDV}^{\mathrm{T}}=\begin{pmatrix} u_{11} & \cdots & u_{1N} \\ \vdots & \ddots & \vdots \\ u_{M1} & \cdots & u_{MN} \end{pmatrix}\begin{pmatrix} d_1 & & 0 \\ & \ddots & \\ 0 & & d_N \end{pmatrix}\begin{pmatrix} v_{11} & \cdots & v_{1N} \\ \vdots & \ddots & \vdots \\ v_{N1} & \cdots & v_{NN} \end{pmatrix}^{\mathrm{T}} \tag{4}$$

$$\mathbf{U}^{\mathrm{T}}\mathbf{U}=\mathbf{I} \qquad \mathbf{V}^{\mathrm{T}}\mathbf{V}=\mathbf{V}\mathbf{V}^{\mathrm{T}}=\mathbf{I} \tag{5}$$

The matrices **U**, **D**, **V** and **I** in Eq. (4) and Eq. (5) have the following meanings.

The matrix **U**: The columns of **U** are the left singular vectors that consist orthogonal basis, where u_{ij} represents seismic intensity at the site i in Mode j. The left singular vector represents the modal form that defines the spatial correlation in a set of seismic intensity distributions. Map of the left singular vector visualizes the spatial correlation between different sites.

The matrix **D**: The dialog matrix whose diagonal entries d_j is the singular value which is equivalent to the square root of eigenvalue in Mode j. The singular value represents the case-independent weight for each mode.

The matrix **V**: The columns of **V** are the right singular vectors that consist orthogonal basis, where v_{ij} is the weight of Mode j in case i. The right singular vector represents the case-dependent weight for each mode, and provides a clue to the interpretation of the modal factor.

The matrix **I**: $N\times N$ identity matrix.

The matrix **UD** represents fundamental structure dominating all cases of seismic intensity distributions and their spatial correlation. Based on the fundamental structure, the seismic intensity distribution of Case i is characterized by the right singular vector which is a column vector of the matrix **V**.

3. Numerical Examples for Mode Decomposition of Scenario Shaking Maps

3.1 Source parameter settings

Table 1 and Fig.1 show source parameters and fault models and their parameters for the two kinds of scenario earthquakes, respectively. The South Western segment of the main part of the Yamasaki Fault Zone (hereafter referred to as “Yamasaki”) and the Central North segment of Fault Zone of the Itoigawa-Shizuoka Tectonic Line (hereafter referred to as “Itoigawa”)

3.1.1 The South Western segment of the main part of the Yamasaki Fault Zone

Yamasaki is a left-lateral strike-slip fault that is modeled by a single element fault with a dip angle of 90 degrees. Four fault rupture scenarios are assumed in accordance with combination of location of the asperities arrangement and hypocenter for Yamasaki.

3.1.2 The Central North segment of Fault Zone of the Itoigawa-Shizuoka Tectonic Line

Itoigawa is also a left-lateral strike-slip fault, but its dip angle is 70 degrees. Itoigawa is modeled using three-element faults. Eight fault rupture scenarios are assumed for Itoigawa.

Table 1 –Source parameters for scenario earthquake (Based on Ref. [2])

	The South Western segment of the main part of the Yamasaki Fault Zone	The Central North segment of Fault Zone of the Itoigawa-Shizuoka Tectonic Line
Type of Fault	Left-lateral strike-slip fault	Left-lateral strike-slip fault
Number of Setting Cases: N	4	8
Number of grid cells: M	125,439	208,024
Number of Element Faults	1	3
Number of Asperities	2	4
Fault Strike	N309.3°E	North : N339.2°E Middle : N330.9°E South : N304.6°E
Fault Dip [°]	90	70
Length [km]	32	North : 34 Middle : 6 South : 8
Width [km]	18	10
Seismic Moment, M_0[Nm]	1.92×10^{19}	3.97×10^{19}
Moment Magnitude Scale, M_w	6.8	7.0

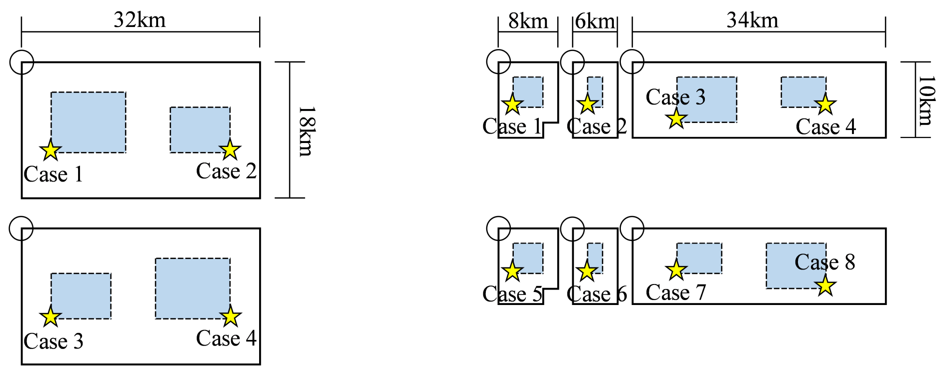

(a) The South Western segment of the main part of the Yamasaki Fault Zone

(b) The Central North segment of Fault Zone of the Itoigawa-Shizuoka Tectonic Line

Fig. 1 - Fault model for scenario earthquake (Based on Ref. [2])

3.2 Seismic Intensity Distributions and Ground Structure

Fig.2 shows the JMA seismic intensity distributions which can be potentially caused by Yamasaki and Itoigawa, and the distributions of the mean and standard deviation value of *N* cases of seismic intensity distributions. However, seismic intensity distributions are shown only for Cases 1-4 out of all *N* cases due to the limitation of space. All seismic intensity maps are evaluated by 250m square grid cells; black solid (or broken) line is the surface fault plane (or the trace of surface fault) and open circle is the origin of the fault plane. Fig.3 shows the site amplification factor (250m square grid cells) and the deep subsurface structure (1km square grid cells) as ground structure in the object range, respectively.

3.2.1 The South Western segment of the main part of the Yamasaki Fault Zone

The regions of seismic intensity 5.5 or greater distribute near southern the fault and the southern of the fault. In Case 2 and 4 that the hypocenter is located in northwestern part of the fault, high seismic intensity distributes in southeastern part of the map due to the forward directivity effect. The standard deviation is large in northwestern part of the map and above the fault. The distribution of the standard deviation is almost line symmetry distributions with the trace of surface fault as an axis, and the possible cause of its characteristic distribution is the strike-slip fault with a dip angle of 90 degrees.

3.2.2 The Central North segment of Fault Zone of the Itoigawa-Shizuoka Tectonic Line

The regions of seismic intensity 5.5 or greater except for Case 4 and 8 that the hypocenter is located in northern part of the northern fault distribute from the surface fault plane to north on the map. In Case 4 and 8, its region distributes from the surface fault plane to the southeastern part of the map. The maximum value of the standard deviation is over twice as large as Yamasaki's, and the variation between cases is remarkable. The standard deviation is especially large from both the northern and southern edge of the fault to northern and southern part of the map, respectively. The deep subsurface structure is especially deep from northern edge of the fault to northeastern on the map; its structure seems to have a great effect on the distributions of both seismic intensity and standard deviation.

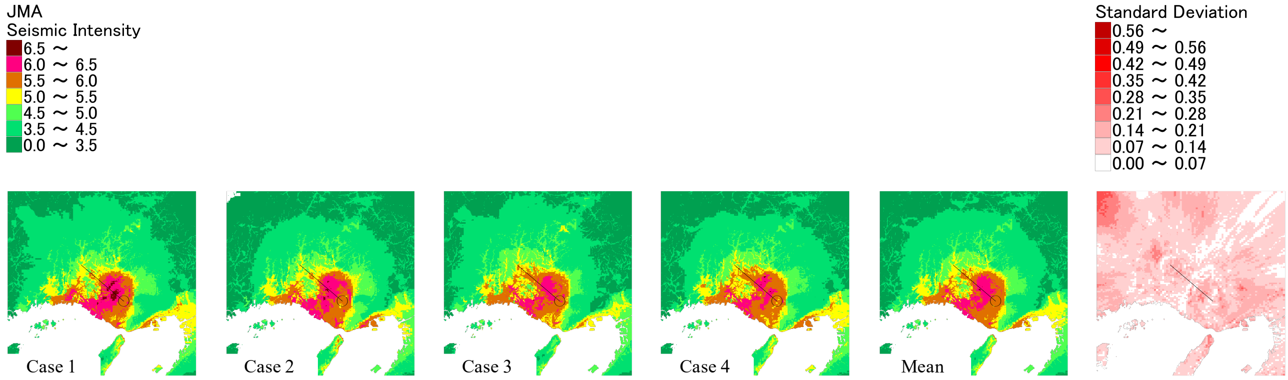

(a) The South Western segment of the main part of the Yamasaki Fault Zone

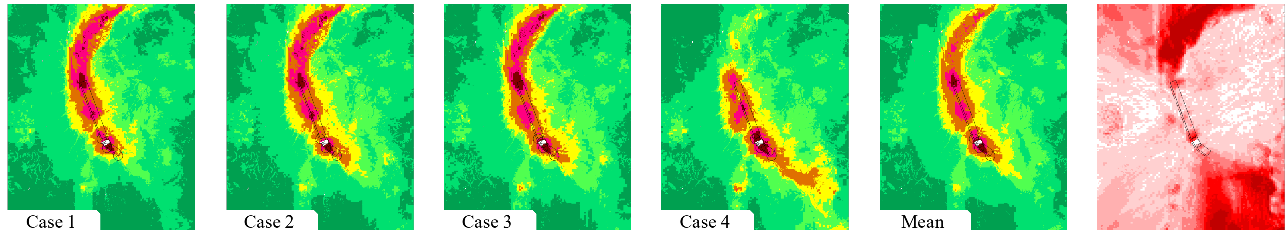

(b) The Central North segment of Fault Zone of the Itoigawa-Shizuoka Tectonic Line

Fig. 2 – Distribution maps of JMA seismic intensity for scenario earthquake, and distribution maps of mean and standard deviation of JMA seismic intensity for *N* cases. (Based on Ref. [2])

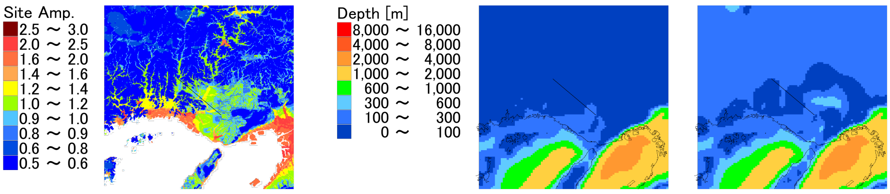

(a) The South Western segment of the main part of the Yamasaki Fault Zone

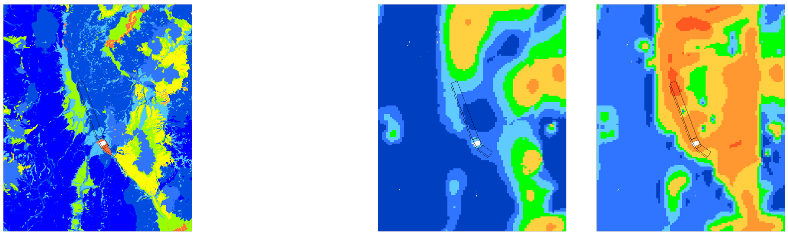

(b) The Central North segment of Fault Zone of the Itoigawa-Shizuoka Tectonic Line

Fig. 3 – Site amplification factor (left) and deep subsurface structure (middle, right: Vs=1700m/s, 2700m/s layer's lower surface) (Based on Ref. [2])

3.3 Mode Decomposition and Evaluate Spatial Correlation

The seismic intensity distributions of N cases are decomposed to the N modes (Yamasaki: N=4, Itoigawa: N=8) by use of mode decomposition. Fig.4 shows the singular values representing diagonal entry of the matrix **D**, and Fig.5 shows the cumulative contribution ratio of eigenvalues which are square of the singular values. In both Yamasaki and Itoigawa, the singular value for Mode 1 is large and the contribution rate is over 90%. The contribution ratio of Mode 2 or higher is not negligible. Especially in Itoigawa, the contribution ratio for Mode 2 is approximately 6.8%, which is considerably larger than that in Yamasaki.

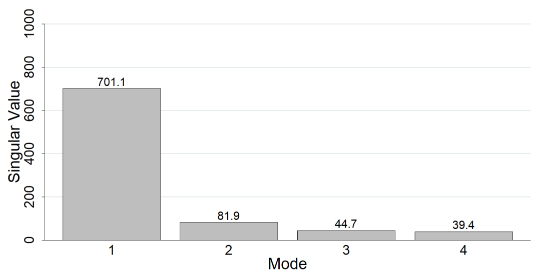

(a) The South Western segment of the main part of the Yamasaki Fault Zone

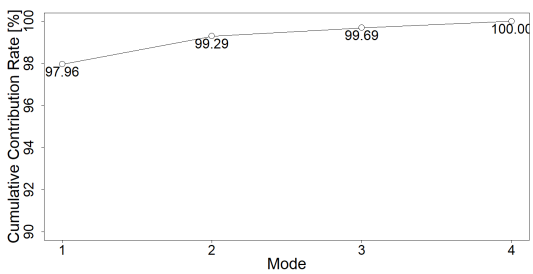

(a) The South Western segment of the main part of the Yamasaki Fault Zone

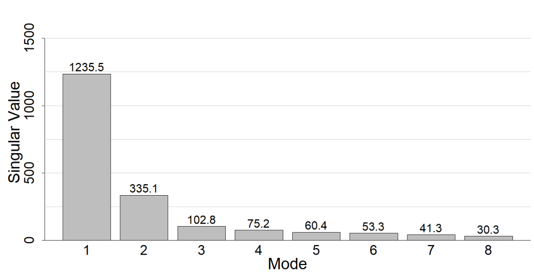

(b) The Central North segment of Fault Zone of the Itoigawa-Shizuoka Tectonic Line

Fig. 4 -Singular value for each mode

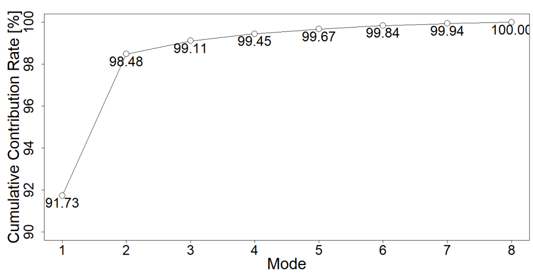

(b) The Central North segment of Fault Zone of the Itoigawa-Shizuoka Tectonic Line

Fig. 5 - Cumulative contribution ratio of eigenvalue

Fig.6 shows the distributions of the left singular vector (the columns of the matrix **U**) for each mode, and Fig.7 shows the right singular vector (the columns of the matrix **V**) for each mode. Only Mode 1-4 for each fault are shown due to the limitation of space. The distributions of the left singular vector (Fig.6) visualizes the spatial correlation between different sites in N cases of seismic intensity distributions. In Fig.6, red grid is positive value and blue grid is negative value; correlation between grids with the same (or different) sign is positive (or negative) correlation. The right vectors (Fig.7) represent the case dependent weight for each mode. The characteristic for each mode is analyzed by relating to the left singular vector, the right singular vector and the source parameters.

3.3.1 The South Western segment of the main part of the Yamasaki Fault Zone [7]

In all modes, the distributions of the left singular vectors are shown almost line symmetry distributions with the trace of surface fault as an axis. However, the distributions are not perfectly symmetrical due to ground structure. Its distribution tendency can only be seen in Yamasaki, and the possible cause of its tendency is the strike-slip fault with a dip angle of 90 degrees.

(1) Mode 1: In the distribution of the left singular vector, positive values are near the fault, and negative values are far away from the fault; the modal form is similar to the mean seismic intensity distribution. The values of the right singular vector are negative and approximately equal in all cases. Thus, Mode 1 represents the characteristic distributions of mean seismic intensity reflecting the attenuation effect due to source-to-site distance. The small differences between cases represents subtle difference in the attenuation effect.

The values of the left singular vector are different in every 250m grid cell. Thus, Mode 1 represents the amplification effect of surface ground that is modeled in 250m grid cells. By contrast, the values of the vector for Mode 2 or higher are basically different in every 1km grid cells. Thus, the effect of deep subsurface structure that is modeled in 1km grid cells, would be reflected in Mode 2 or higher, but the effect does not appear in Yamasaki.

(2) Mode 2: In the distribution of the left singular vector, positive (or negative) values are in the northwestern (or southeastern) part of the map; area distributing positive and negative values are spatially divided into two. The positive (or negative) values of the right singular vector are in Case 1 and 3 (or Case 2 and 4) that the hypocenter is located in southeastern (or northwestern) part of the fault. Thus, Mode 2 represents the forward directivity effect depending on the location of the hypocenter. In Mode 2, spatial correlation between a pair of two sites located in the same direction with regard to rupture propagation shows positive correlation. On the country, a pair of two sites located in the opposite direction shows negative correlation.

(3) Mode 3: In the distribution of the left singular vector, positive (or negative) values are near northwestern (or southeastern) part of the fault. Negative and positive areas alternately distribute from northwest to southeast on the map. The positive (or negative) values of the right singular vector are in Case 3 and 4 (or Case 1 and 2) that the larger asperity lies northwest (southeast) of the fault. Thus, Mode 3 represents the arrangement setting of the larger asperity.

(4) Mode 4: The distribution of the left singular vector is more complicated than that of the Mode 1-3, and the relation with the source parameter settings cannot be seen. Thus, Mode 4 is the fine adjustment term of seismic intensity distribution for each case. The modal form of higher mode shows complicated spatial correlation, and its tendency is also observed in Itoigawa.

3.3.2 The Central North segment of Fault Zone of the Itoigawa-Shizuoka Tectonic Line [7]

(1) Mode 1: Mode 1 represents the attenuation effect and the amplification effect of surface ground, as in Yamasaki. In addition, since values of the left singular vector in northern part of the map where the deep subsurface structure is especially deep show large positive values, Mode 1 also represents the effect of the deep subsurface structure.

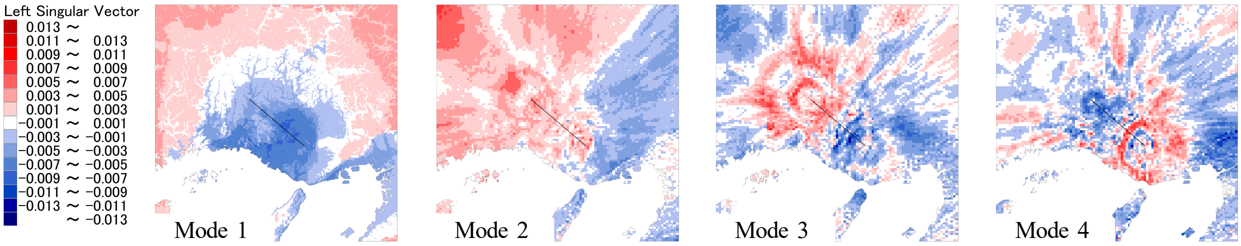

(a) The South Western segment of the main part of the Yamasaki Fault Zone

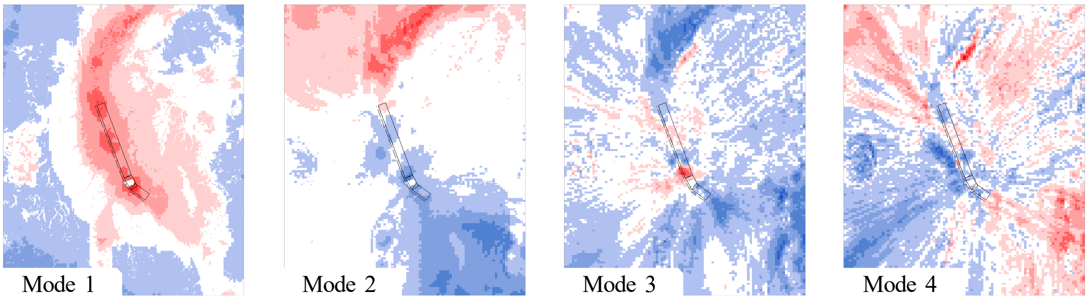

(b) The Central North segment of Fault Zone of the Itoigawa-Shizuoka Tectonic Line

Fig. 6 – Distribution of left singular vector (column vector of matrix **U**) for each mode

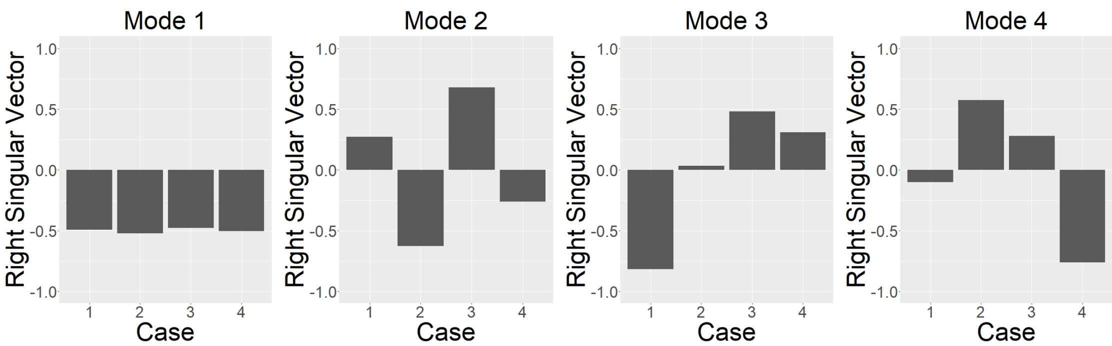

(a) The South Western segment of the main part of the Yamasaki Fault Zone

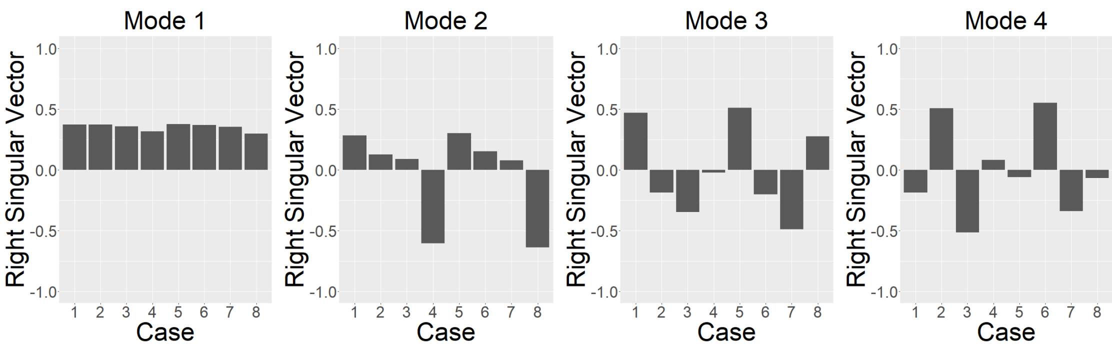

(b) The Central North segment of Fault Zone of the Itoigawa-Shizuoka Tectonic Line

Fig. 7 – Right singular vector (column vector of matrix **V**) for each mode

(2) Mode 2: In the distribution of the left singular vector, positive (or negative) values are in north on the map (or near the fault); area showing positive and negative correlation are extremely clearly divided into two. The negative values of the right singular vector are in Case 4 and 8 that the hypocenter is located in northern part of the northern fault, and positive values are in all cases except Case 4 and 8. Thus, Mode 2 represents the forward directivity effect depending on the location of the hypocenter. In addition, since values of the left singular vector in the northern on the map show large positive values, the deep subsurface structure also affects Mode 2. As shown in Fig.5 (b), the contribution ratio for Mode 2 is approximately 6.8%, which is much large than that of Yamasaki (approximately 1.3%).

(3) Mode 3: Negative values of the left singular vector are dominant entire the map, while positive values are in the middle of the map and large positive values are concentrated near the southern edge of the northern fault. In the right singular vector, each pair of Case 1 and 5, Case 2 and 6, and Case 3 and 7 take the similar value, respectively. Thus, Mode 3 represents the forward directivity effect depending on the location of the hypocenter, and the effect of simultaneous arrival of waves from several asperities. However, it is difficult to analyze the modal form. Negative values of the left singular vector in north on the map show the influence of the deep subsurface structure as well as Mode 1 and 2.

(4) Mode 4: In the distribution of the left singular vector, positive (or negative) values are in north and southeast on the map (or from the southern edge of the northern fault to southwest on the map). The positive values of the right singular vector are in Case 2 and 6 that the hypocenter is located in the middle fault, and negative values are in Case 3 and 7 (or Case 1 and 5) that the hypocenter is located in the northern (or southern) fault. It is difficult to analyze the modal form, but Mode 4 is affected by the forward directivity effect and the effect of simultaneous arrival of waves from several asperities as well as Mode 3.

3.3.3 Comparison of modal characteristic

Table 2 summarizes the modal characteristics of spatial distribution trend and dominant factor for each scenario earthquake maps. For reference, Mode 5-8 omitted in this paper are also described in Table 2. In Yamasaki and Itoigawa, the characteristics for Mode 1 and 2 are similar. Mode decomposition reveals that the forward directivity effect greatly affects *N* cases of scenario shaking map.

Table 1 – Modal characteristic for scenario shaking maps

<table>
<tr><th></th><th colspan="2">The South Western segment of the main part of the Yamasaki Fault Zone (Dip Angle 90°, N=4)</th><th colspan="2">The Central North segment of Fault Zone of the Itoigawa-Shizuoka Tectonic Line (Dip Angle70°, N=8)</th></tr>
<tr><td>Mode 1</td><td colspan="4">Characteristic distributions of mean seismic intensity (Attenuation effect due to source-to-site distance, amplification effect of subsurface ground)</td></tr>
<tr><td>Mode 2</td><td>Forward directivity effect</td><td rowspan="3">Almost line symmetry distributions with the trace of surface fault as an axis</td><td>Forward directivity effect</td><td rowspan="2">Effect of deep subsurface structure</td></tr>
<tr><td>Mode 3</td><td>Arrangement setting of the larger asperity</td><td>Effect of simultaneous arrival from several asperities (+ Forward directivity effect)</td></tr>
<tr><td>Mode 4</td><td>Fine adjustment term of seismic intensity distribution for each case</td><td colspan="2">Effect of simultaneous arrival from several asperities (+ Forward directivity effect)</td></tr>
<tr><td>Mode 5</td><td colspan="2" rowspan="2"></td><td colspan="2">Bias in gravity center of asperities (from the right singular vector)</td></tr>
<tr><td>Mode 6-8</td><td colspan="2">Fine adjustment term of seismic intensity distribution for each case</td></tr>
</table>

4. Simulation of Strong Ground Motion Distribution by Mode Synthesis

4.1 Simulation of Strong Ground Motion Distribution Considering Spatial Correlation

As mentioned in **2**, the matrix **UD** obtained by using singular value decomposition is fundamental structure dominating all cases of seismic intensity distributions, and the right singular vector which is a column vector of the matrix **V**, represents features for each case and mode. Therefore, by simulation replacing the right singular vector for another *N*-dimensional vector while keeping **U** and **D,** and synthesizing orthogonal mode, strong ground motion distribution preserving the spatial variation and correlation in original set of shaking maps is generated [6]. Here, this study employs statistical preconditioning [8] as a simulation method, as in the previous study [6]. In statistical preconditioning, the periodicity and collocation orthogonality of the cosine function are utilized, and the result exactly satisfies the orthogonality. The number of trials of its method is $S = 4NN_f$, and N_f represents a total number of superimposed cosine functions.

The $S \times N$ matrix **W** composed of *N*-dimensional vectors for *S* cases by use of statistical preconditioning replaces the $N \times N$ matrix **V** in Eq. (4), and mode synthesis is applied to **UD** and **W** as follows.

$$\mathbf{Y_0} = \mathbf{UDW}^{\mathrm{T}} \tag{6}$$

S cases of simulated seismic intensity distributions are obtained from the matrix $\mathbf{Y_0}$ as follows.

$$\mathbf{Y} = \mu_G \mathbf{H}' + \sigma_G \mathbf{Y_0} \tag{7}$$

where **H'** is the $M \times S$ matrix in which all of the entries are 1.

4.2 Simulated Strong Ground Motion Distributions

In this study, the total number of superimposed cosine functions was set to N_f =4, and simulated seismic intensity distributions were generated 64 and 128 cases in Yamasaki and Itoigawa, respectively (Fig. 8). Simulated seismic intensity distributions show similar tendencies to scenario shaking maps.

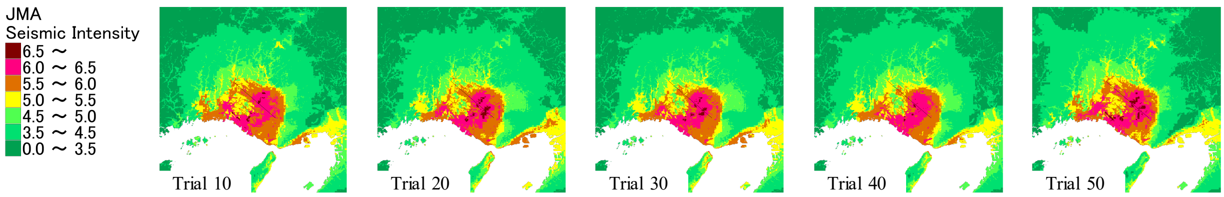

(a) The South Western segment of the main part of the Yamasaki Fault Zone

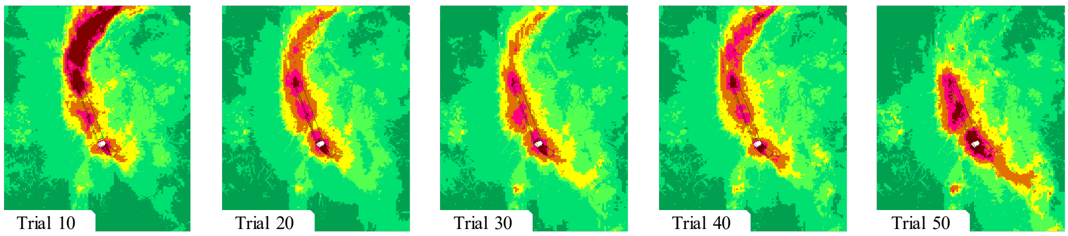

(b) The Central North segment of Fault Zone of the Itoigawa-Shizuoka Tectonic Line

Fig. 8 – Some simulated JMA seismic intensity distribution maps

Correlation of seismic intensity among 27 selected points (Fig. 9) where are measured mean seismic intensity of 4.5 or greater by Itoigawa's scenario shaking maps is shown in Fig. 10. Fig. 10 reveals that the simulation method is capable of generating an arbitrary number of cases of seismic intensity distributions maps preserving the spatial variation and correlation in original set of shaking maps. Spatial correlation between a pair of two sites located in the same direction with regard to rupture propagation, e.g. Point 15 and Point 17, shows positive correlation. In contrast, a pair of two sites located in the opposite direction, e.g. Point 5 and Point 17, shows negative correlation. Therefore, correlation between sites in Itoigawa is dominantly attributed to the above-mentioned Mode 2 representing spatial correlation due to the forward directivity effect. In addition, site-to-site correlation in Yamasaki (abbreviated in the figure) also is dominantly attributed to Mode 2 that is related to the forward directivity effect. The simulation method can be conveniently used for damage and risk assessment requiring a large number of seismic intensity distributions taking spatial correlation into account.

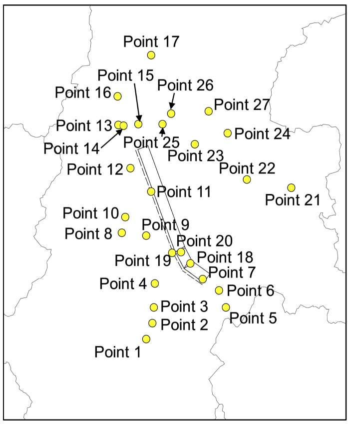

Fig. 9 - Location of 27 selected points in Itoigawa

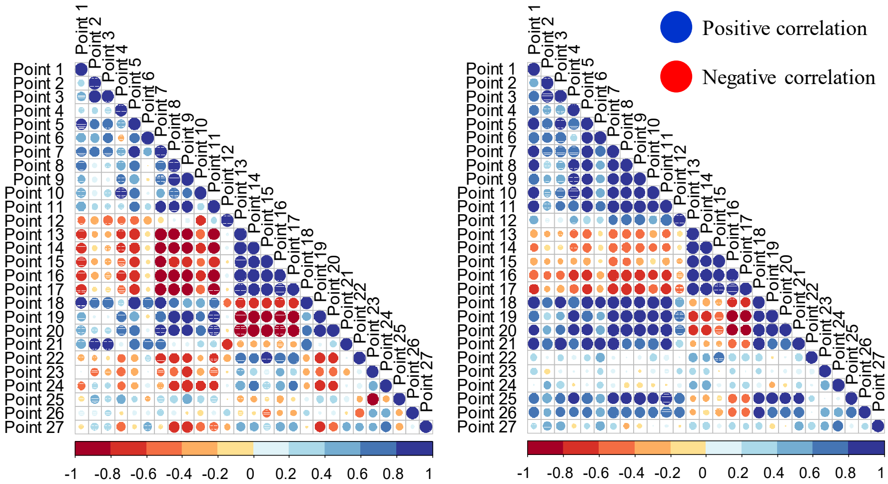

(a) Scenario shaking maps (8 cases)

(b) Simulated seismic intensity maps (128 cases)

Fig. 10 – Correlations of seismic intensity among selected points in Itoigawa

5. Conclusions and future developments

The major conclusions derived from this study are listed below.

(1) The mode decomposition method based on singular value decomposition [6] was applied seismic intensity distributions for scenario earthquakes to evaluate spatial variation and correlation reflected in a set of seismic intensity distributions. This study used two kinds of scenario earthquakes with can be potentially caused by strike-slip faults: the South Western segment of the main part of the Yamasaki Fault Zone and the Central North segment of Fault Zone of the Itoigawa-Shizuoka Tectonic Line.

(2) Spatial variation and correlation of Mode 1 represents the characteristic distributions of mean seismic intensity reflecting the attenuation effect due to source-to-site distance and amplification effect of subsurface ground. Spatial variation and correlation of Mode 2 represents the forward directivity effect, and the contribution ratio in Itoigawa is an especially large number. These tendencies observed in Mode 1 and 2 are common to two scenario earthquakes of strike-slip faults. The higher modes show complex spatial correlation, and different tendencies are observed for two scenario earthquakes.

(3) By synthesizing orthogonal modes obtained using singular value decomposition, Monte Carlo simulations generating a number of seismic intensity distributions preserving the spatial variation and correlation in original shaking maps [6] were performed. Site-to-site correlation in simulation seismic intensity distributions were found to be dominantly to Mode 2 representing spatial correlation with regard to forward directivity effect.

For future developments, we plan to the simulated apply the simulated seismic intensity distributions to seismic risk of spatially distributed networks or portfolio risk of an inventory of buildings.

6. Acknowledgements

This study used JMA seismic intensity distributions for scenario earthquakes published by the Headquarters for Earthquake Research Promotion [1] and Seismic Hazard Information Site (J-SHIS) [2] established by the National Research Institute for Earth Science and Disaster Resilience. The authors gratefully acknowledge them.

7. References

[1] The Headquarters for Earthquake Research Promotion (2018): National seismic hazard maps for Japan (2018), https://www.jishin.go.jp/evaluation/seismic_hazard_map/shm_report/shm_report_2018/ (in Japanese) [accessed February 3rd, 2020]

[2] The National Research Institute for Earth Science and Disaster Resilience (NIED): Japan seismic hazard information station (J-SHIS): http://www.j-shis.bosai.go.jp/en/ [accessed February 3rd, 2020]

[3] Takada T, Shimomura T (2003): Macro-spatial correlation of seismic ground motion on strong motion records of the 1999 Chi-Chi earthquake. *Journal of Structural and Construction Engineering*, **68** (566), 41-48 (in Japanese)

[4] Hayashi T, Fukushima S, Yashiro H (2006): Effects of the spatial correlation between ground motion intensities on the seismic risk of portfolio of buildings, **71** (600), 203-210 (in Japanese)

[5] Park J, Bazzurro P, Baker JW (2007): Modeling spatial correlation of ground motion intensity measures for regional seismic hazard and portfolio loss estimation, *Proceedings of the 10th international conference on Application of Statistic and Probability in Civil Engineering*, Tokyo, Japan, 1-8.

[6] Nojima N, Kuse M, Quang LD (2018): Mode decomposition and simulation of strong ground motion distribution using singular value decomposition, *Journal of Japan Association for Earthquake Engineering*, **18** (2), 95-114 (in Japanese)

[7] Nojima N, Kuse M, Takahashi Y (2019): Analysis of spatial variation and correlation of predicted seismic intensity maps for scenario earthquake by use of mode decomposition, *Journal of Japan Association for Earthquake Engineering*, **19** (1), 121-135 (in Japanese)

[8] Yamazaki F, Shinozuka M (1990): Simulation of stochastic fields by statistical preconditioning, *Journal of Engineering Mechanics*, **116** (2), 268-287.

